



Acclimation dynamics of *Chlorella vulgaris* to sudden light change

Arthur Oliver ^{*}, Patrick Perré, Victor Pozzobon

Université Paris-Saclay, CentraleSupélec, Laboratoire de Génie des Procédés et Matériaux, Centre Européen de Biotechnologie et de Bioéconomie (CEBB), 3 rue des Rouges Terres, 51110 Pomacle, France



ARTICLE INFO

Keywords:

Microalgae
Acclimation
Chlorophyll
Light
Light shift

ABSTRACT

Chlorella vulgaris photoacclimation was monitored over eight instantaneous light intensity changes. The intensities ranged between $35 \mu\text{mol Photon}_{\text{PAR}} \cdot \text{m}^{-2} \cdot \text{s}^{-1}$ and $600 \mu\text{mol Photon}_{\text{PAR}} \cdot \text{m}^{-2} \cdot \text{s}^{-1}$. Cultures were grown in ultra-thin flat panel photobioreactors under continuous light and maintained in low cell density to ensure homogeneous light availability. Photoacclimation was evaluated through spectral quantification of pigments and fluorometric assays. The former gave access to a proxy of chlorophyll and carotenoid content, the latter to the Photosystem-II cross-section (σ_{PSII}) and qualification of the photosynthetic machinery (via OJIP assays). Both the acclimated steady-state values of pigment content and the dynamic of their evolutions after sudden light intensity change were monitored. The characteristic times of the transitions were estimated based on a first-order assumption. Results consistently showed that antenna size adjustment of *Chlorella vulgaris* was primarily dictated by the light availability, both regarding the acclimated steady-state values and the acclimation dynamics. An energetic limitation was highlighted by the acclimation dynamics at low light. The characteristic time of transition was estimated to be $16.6 \pm 2.17\text{h}$ for the transition to the lowest light intensity ($35 \mu\text{mol Photon}_{\text{PAR}} \cdot \text{m}^{-2} \cdot \text{s}^{-1}$) and $3.55 \pm 1.01\text{h}$ for intensities higher than the maximal intensity of photo-limitation ($120 \mu\text{mol Photon}_{\text{PAR}} \cdot \text{m}^{-2} \cdot \text{s}^{-1}$). No hysteresis effect was observed as light intensities were shifted once and reverted to their original values. These results extend the literature regarding photoacclimation dynamics of antenna size and photosynthetic apparatus. They are well-suited to calibrate photoacclimation models and can provide valuable insight into the strategies to implement for culture scale-up, fed-batch, and semi-continuous processes.

1. Introduction

The culture of microalgae for biotechnological purposes has known important growth over the last decades, especially because of its high potential in terms of production of high-added value molecules (in cosmetics, pharmaceuticals, and the nutraceutical field [1,2]), and the ecosystemic benefits associated with their growth, such as water decontamination [3]. Other applications include animal feed - notably in aquaculture [4] - and human nutrition [5]. Photoautotrophic growth is in many cases the most suited solution, as, in addition to CO₂ capture, it provides specimens of better quality, especially for the production of pigments, naturally associated with the photosynthetic apparatus of microalgae [6], for costs comparable to heterotrophic growth [7].

Despite a high potential and promising laboratory results, the sector of green microalgae struggles to overcome its limitations, mostly related to the scale-up processes [8,9]. The main constraint in photoautotrophic cultures is undoubtedly the light availability inside traditional

photobioreactors (PBR) [10,11]. As cultures grow denser, the aphotic zone of the PBR expands, and volumetric productivity declines. Inversely, increasing the incident light limits the aphotic zone but heightens the risks of photodamage near the wall of the PBR. This is a complex tradeoff that must be addressed for the design of photobioreactors and the development of illumination and agitation strategies [12,13]. Many studies have focused on this topic, especially in the design of photobioreactors to optimize light distribution, either in terms of shape [10,12,14] or strategically positioned additional light sources [15,16]. In particular, the mixing of the cultures generates patterns of intermittent light of frequencies ranging between 0.1 Hz and 100 Hz, which are difficult to control [17]. The impact of these light patterns on the growth and pigmentation of green microalgae has also been widely investigated [18–20].

It is now well known that microalgae can acclimate to different illuminations, primarily by adjusting their pigmentation [21]. The amount of light-harvesting pigments (chlorophyll *a* and *b*, or primary

* Corresponding author.

E-mail address: arthur.oliver@centralesupelec.fr (A. Oliver).

carotenoids such as β -carotene or lutein) in acclimated states depends on the illumination and other substrate availability [22–24]. This modulation serves either a change in the antenna size (σ -strategy) or in the number of PhotoSynthetic Units (N -strategy) [25]. In addition, photo-protective mechanisms involve modulation of the carotenoid content, mainly to dissipate excess energy through Non-Photochemical Quenching (NPQ) or Reactive Oxygen Species (ROS) scavenging [26–28].

To the best of the authors' knowledge, the dynamic of microalgal acclimation to a light change within hours to days was significantly less addressed than the characterization of their acclimated states. The investigation of acclimation dynamics also differs from the one of the influence of photoperiod that mimics natural sunlight (including a period without light) and focuses on steady-state parameters after a few days [29,30]. Most studies related to the subject investigate a limited number of intensities and transitions between them. Besides, the parameters used to study the acclimation are biologically relevant but often present limited applicability from a biotechnological standpoint. Fisher et al. studied the dynamic of the ultrastructure changes in *Nannochloropsis* sp. in a light shift between High Light (HL) and Low Light (LL) [31]. Shapira et al. studied the acclimation of the inverse shift (LL to HL) for *Chlamydomonas reinhardtii*, focusing mostly on consequent gene expression [32]. Straka and Rittman performed a similar analysis on both shifts, mostly focused on growth, with the cyanobacteria *Synechocystis* sp. [33]. These studies conclude with different characteristic times of photoacclimation. In addition, these studies are too dissimilar (different strains, intensities, and nature of parameters studied) and the data too scarce to identify the source of the discrepancies.

Overall, the lack of data remains substantial in this domain, especially considering the wide range of intensities used in microalgae culture and the complexity of the acclimation mechanisms. Notably, no relation between the dynamic of acclimation and the light intensity has been established. Similar observations apply to the potential presence of a hysteresis regarding the acclimated states, as most studies focus on light transitions as isolated events. A better characterization of these phenomena could help the design of photobioreactors, as well as illumination and agitation strategies, notably in the case of dense cultures [34].

The main objective of this article is to extend the knowledge of the photoacclimation dynamics of green microalgae by investigating changes between multiple illumination levels. To this end, the main parameter monitored was chlorophyll content. Additional assessments of the photosynthetic apparatus status through fast fluorescence protocols were performed. The transitions were defined based on the classical PI curve to be representative of the different light regimes. The reference microalgae *Chlorella vulgaris* was grown in ultra-thin flat panel photobioreactors with an automated optical density control to guarantee an optically thin culture and a homogeneous light availability inside the photobioreactors. This protocol allowed the dynamic of acclimation of the microalgae to be visualized and the characteristic time needed to adjust to new conditions to be identified. This information is intended to help parameterize photoacclimation models [35,36], to represent the consequent evolution of light availability inside a PBR [37], and to investigate the consequences of slow agitation in dense cultures.

2. Materials and method

2.1. Strain, growth medium, and subculturing

Chlorella vulgaris (211–12) was purchased from the Culture Collection of Algae at Gottingen University (SAG). The cells were grown in an enriched B3N medium derived from BBN as described in [38]. The medium was stored at 4 °C in the dark. Subcultures were realized every two weeks in 250 ml Erlenmeyer flasks by inoculating 5 ml of culture

into 50 ml of fresh medium. Flasks were placed on an orbiting platform at 25 °C and low light (around 50 $\mu\text{mol Photon}_{\text{PAR}} \cdot \text{m}^{-2} \cdot \text{s}^{-1}$).

2.2. Experimental setup

The installation is represented in Fig. 1. The experiments were realized in a flat panel photobioreactor with a V-shaped base, a 135 mL working volume, and a 6 mm width. The light was provided using computer-controlled LED panels. The cultures were placed into an aluminum box isolated from exterior light sources. The spatial distribution of light was assessed by measuring the intensity at various positions within the PBR plane (LICOR LI 250 A & LI-190R sensor). This illumination cartography showed that the variation around the average intensity did not exceed 10 % of this value. Three identical PBRs were placed inside the light-deprivation box, constituting a biological triplicate. The cultures were maintained at approximately 25 °C by a heater-chiller system of cooling water and provided with 2.5 % CO_2 -enriched air, bubbling from the bottom (flowrate of 200 $\text{mL} \cdot \text{min}^{-1}$) for growth and mixing purposes.

The cells were grown in a turbidostatic mode to ensure low cell density and subsequent illumination homogeneity. Optical density was measured through an optical fiber connected to a spectrophotometer. Fresh B3N medium was automatically injected into the bioreactors when the optical density exceeded a 0.1 threshold, which correspond to 80 % of the incident illumination retrieved at the back of the PBR. It was chosen to monitor the optical density based on the absorption at 463 nm, which corresponds to the maximal absorption peak of the chlorophyll in the blue region of the visible spectrum. An overflow valve was positioned on the upper part of the PBR to discharge the excess culture. Samples of 4 mL were extracted at various time intervals from a dedicated outlet at the base of each PBR to perform the experimental assays described in the next section.

2.3. Pigment extraction and qualitative assessment

The first assay consisted of a qualitative assessment of the chlorophyll and carotenoid content through spectrophotometric measurement of pigment extracts, based on the work of Porra et al. [39]. Samples of 1 mL were placed with 4 mL of methanol and 1 g of fine sand in 10 mL test tubes. The latter were covered in aluminum foil to prevent light-induced pigment degradation. The cells were crushed with a bead beater (MP Biomedicals FastPrep42), placed for 20 minutes in a 60 °C

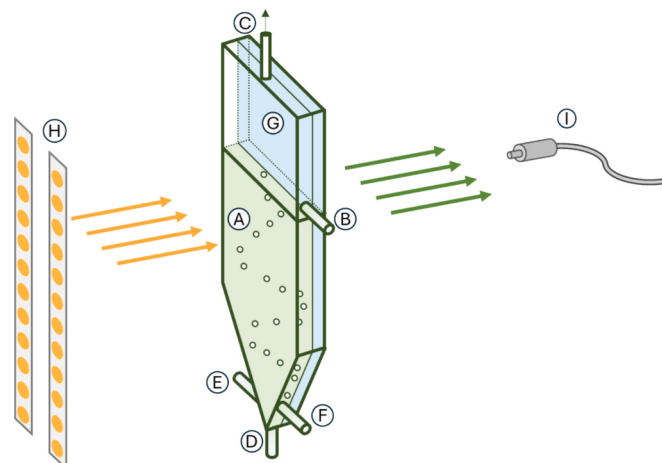


Fig. 1. Experimental installation (only one of the three PBR is represented). A) Culture compartment, B) Overflow valve, C) Vent, D) Gas injection inlet, E) Medium injection inlet, F) Sampling outlet, G) Water-cooling compartment, H) LED panel, I) Optical fiber connected to the spectrophotometer for turbidostatic control.

agitated water bath, and filtered before a spectral acquisition (Shimadzu UV-1800 spectrophotometer) over the visible domain (400 nm – 800 nm, 0.2 nm resolution).

The maximum absorption of chlorophyll in the red (around 665 nm in methanol) was retrieved and divided by the optical density of the whole cells at 750 nm, previously measured as a proxy of the cell concentration. This represented a qualitative estimation of the chlorophyll content per cell. A quantitative value could not be calculated without an accurate estimation of the dry weight or a chromatographic protocol. Both these solutions would have required a higher pigment content, either with a higher cell concentration or a larger sample volume. The first solution would have compromised the low-optical density paramount to ensure illumination homogeneity while the second was not suited to the working volume of the PBR nor to the high sampling rate required to monitor an acclimation dynamic.

The contribution of carotenoids to each spectrum was evaluated through a subtraction method illustrated in Fig. 2. Chlorophyll *a* and chlorophyll *b* spectra in 100% methanol were taken from the PhotochemCAD database [40] (no available data for 80% methanol). The contributions of chlorophyll *a* and *b* to each spectrum were estimated based on the readings between 600 nm and 700 nm, and then extrapolated over the whole visible domain. The spectra of total carotenoids were computed as the difference between the initial spectra and the chlorophyll extrapolation. A proxy of total carotenoid content was estimated as the ratio between the local maximum of the carotenoids around 465 nm and the optical density of the whole cells at 750 nm. The proportion of carotenoids relative to the chlorophyll (R_{cc}) was defined as the ratio of the two proxies of pigment content. It corresponds to the ratio of peaks (465 nm for the carotenoid spectrum and 665 nm for the chlorophyll spectrum).

As mentioned, the method used to obtain the pigment content (chlorophyll and carotenoids) is only qualitative. The main focus of these experiments is to demonstrate how the organisms adapt, so the precise numerical values are not the primary concern. Nevertheless, the method's accuracy was tested by comparing it to another experiment where the pigment content was measured using an HPLC quantification method (Ultima 3000 HPLC, Thermo Fisher Scientific). A linear regression was performed between the results from both methods for total chlorophyll and total carotenoids (lutein, violaxanthin, and zeaxanthin for the HPLC). The coefficients of determination for this study were satisfactory (respectively $R^2 = 0.96$ for the chlorophyll and $R^2 = 0.87$ for the carotenoids) as illustrated in Fig. S1 and Fig. S2.

2.4. Fluorometric measurements

In addition to the pigmentary qualitative assessment, two fluorometric measurements were performed (Dual-Modulation Kinetic Fluorometer FL 6000, Photon System Instrument). The first analysis is

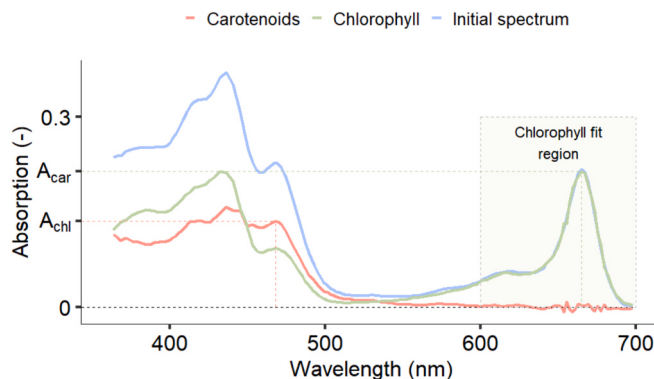


Fig. 2. Spectrum subtraction method. The shaded region highlights the points used to estimate the proportion of chlorophyll *a* and *b*.

inspired by the work of Lavergne and Melis [41–43]. Part of their respective work aims to unravel the properties of *PSI* and *PSII* through fluorometric measurements. They showed that it is possible to estimate the cross-section of *PSII* (σ_{PSII}) by observing the response of a photosynthetic sample to a single turnover flash (a light flash sufficiently short to excite each photosystem no more than once). When exposed to such a flash, photosystems transit from an open to a closed state with a rate described by Eq. (1), where q represents the fraction of open Photosystem II, and I the light intensity. The level of fluorescence measured by the device is linked to the amount of closed photosystem, which makes the identification of σ_{PSII} possible. This method was used for the sake of simplicity to the detriment of some biological subtleties out of the scope of this study.

$$\frac{dq}{dt} = -\sigma_{PSII} I q \quad (1)$$

The second analysis was a transient fluorescence analysis (OJIP) based on the method described by Strasser et al. [44]. Three main parameters were derived from the OJIP. The absorbed energy per reaction center (ABS/RC), the trapped energy per reaction center (TR_0/RC), and the transferred energy per reaction center (ET_0/RC). They respectively provide information on the ability of the antennae to harvest light, the proportion of the light energy converted into electrons by the special pair, and the proportion of electrons effectively transmitted to the Electron Transport Chain. In light of the experiments' nature and the consequent evolution of the number of reaction centers, the indicators were presented per excited Cross-Section (ABS/CS_0 , TR_0/CS_0 , ET_0/CS_0) [44]. The ratio of active reaction centers per excited cross-section was also calculated (RC/CS_0). This cross-section (CS_0) must not be confused with σ_{PSII} defined in Eq. (1). The former relates to the active area of the sampled cells, the latter qualifies the ability of photosystems to close the reaction centers. In particular, CS_0 was not accessible with the OJIP assays. Only ratios between different parameters were available, in arbitrary units. Lastly, the quantum efficiencies of the photosynthetic steps (TR_0/ABS , ET_0/TR_0 , and ET_0/ABS) were calculated. For both fluorometric assays, the samples were kept in the dark for 15 min beforehand to allow the recovery of all photosystems.

2.5. Experiment procedure

First, the cultures were maintained under a constant intensity I_1 for at least 48 h to reach an acclimated state [45]. After this delay, the light was shifted to an intensity I_2 for the same amount of time, before returning to the initial level I_1 . This final stage was monitored for 24 to 48 h depending on the condition, due to restrictions in the accessibility of the equipment. Samples were withdrawn approximately once every hour during the 9 h following a light change, and twice a day otherwise.

For each experiment, the acclimated value of total chlorophyll content for I_1 and I_2 as well as the characteristic time of transition between the two intensities (τ_c) were retrieved. The chlorophyll content of the acclimated state was evaluated either as the value preceding a light change or as the last point of the experiment (when >48 h had passed since the light shift). The characteristic times τ_c were evaluated by fitting the experimental data to an exponential model described by Eq. (2).

$$chl(t) = chl_{t_f} + (chl_{t_0} - chl_{t_f}) e^{-\frac{(t-t_0)}{\tau_c}} \quad (2)$$

With τ_c the characteristic time of the transition, t_0 the instant of the light change, and chl_{t_0} , chl_{t_f} two constants referring respectively to the initial and final chlorophyll content. The value of chlorophyll at t_0 was taken as the value obtained with the preceding sample.

2.6. Illumination conditions

The light intensities were chosen based on an acclimated *PI* curve obtained for *Chlorella vulgaris*, for which no photoinhibition was

identified for intensities as high as $800 \mu\text{mol Photon}_{\text{PAR}} \cdot \text{m}^{-2} \cdot \text{s}^{-1}$ [21]. The trend of the curve and the corresponding levels of chlorophyll are illustrated in Fig. 3. Three empirical zones were defined based on the shape of the curve. A photolimitation zone (P_L) below the photolimitation intensity $I_L = 120 \mu\text{mol Photon}_{\text{PAR}} \cdot \text{m}^{-2} \cdot \text{s}^{-1}$, a zone of photo-saturation in moderate light (P_{SM}) between $120 \mu\text{mol Photon}_{\text{PAR}} \cdot \text{m}^{-2} \cdot \text{s}^{-1}$ and $350 \mu\text{mol Photon}_{\text{PAR}} \cdot \text{m}^{-2} \cdot \text{s}^{-1}$, and a last one of photo-saturation in high light (P_{SH}) over $350 \mu\text{mol Photon}_{\text{PAR}} \cdot \text{m}^{-2} \cdot \text{s}^{-1}$. Transitions between each of the three zones and an additional transition within the first (where the changes are the most contrasted) were performed. The shifts are summarized in Table 1 and illustrated in Fig. 3. The intensities reported correspond to the mean of the incident light measured at the surface of the PBR within the light-deprivation box.

The experiments were designed to allow the observation of the reverse photoacclimation dynamics. The light was shifted once and restored to its original value. This strategy was elaborated to highlight a potential hysteresis effect in the acclimation mechanisms of the microalgae. One condition (N°2 in Table 1) had to be performed in two separate experiments, so the evaluation of the hysteresis effect was realized on the three remaining conditions. The OJIP assays were only realized for two conditions (N°3&N°4 in Table 1). The first condition presented the greatest intensity change, while the second was within the most critical zone (P_L). To simplify the notations, the lower light intensity in one experiment will be referred to as LL and the higher as HL. Depending on the second intensity involved in the condition, $120 \mu\text{mol Photon}_{\text{PAR}} \cdot \text{m}^{-2} \cdot \text{s}^{-1}$ will then be referred once as LL and once as HL (see Table 1).

2.7. Statistical analysis

The results are presented as the mean of replicates ($n = 3$), while the error bars represent the standard deviations. When assessing the equality of indicators over different conditions, Bartlett tests of variance were performed. For conditions with equal variances ($p < 0.05$), ANOVA tests were realized (the condition of mean equality was tested with $p < 0.05$). Models were fitted with a particle swarm optimization (PSO) algorithm ($N_{\text{particle}} = 40$, $\omega = 0.72$, $c_1 = c_2 = 1.19$). Error distributions were assessed with a Shapiro-Wilk test of normality. For $p > 0.05$, the null hypothesis of normally distributed populations was not rejected. In this case, the most likely normal distribution $\mathcal{N}(\mu, \sigma^2)$ of the error was estimated. If the interval $[\mu - \sigma, \mu + \sigma]$ contained 0, the error was considered normal and zero-centered.

3. Results

The evolution of chlorophyll over time enabled the analysis of the acclimation dynamics regarding the light-harvesting ability. Contrasted changes in chlorophyll content were observed for all light shifts. The

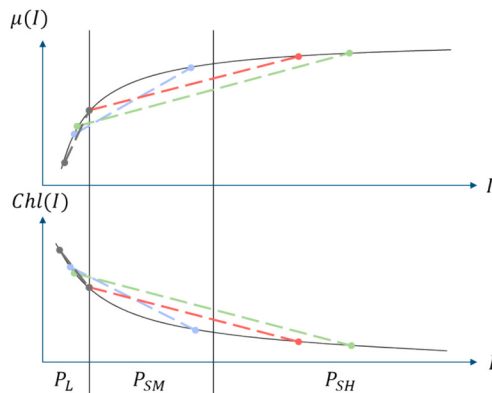


Fig. 3. Illustration of the zones of the PI curve and the light shifts of the study.

Table 1
Summary of the light shifts realized in the study.

N°	I_1 (LL) ($\mu\text{mol Photon}_{\text{PAR}} \cdot \text{m}^{-2} \cdot \text{s}^{-1}$)	I_2 (HL) ($\mu\text{mol Photon}_{\text{PAR}} \cdot \text{m}^{-2} \cdot \text{s}^{-1}$)	Zone 1	Zone 2
1	50	300	P_L	P_{SM}
2	120	500	P_{SM}	P_{SH}
3	65	600	P_L	P_{SH}
4	35	120	P_L	P_L'

fluorometric assays coupled with the pigment modulation granted further insight into the acclimation strategies, especially regarding the most extreme shifts (between $65 \mu\text{mol Photon}_{\text{PAR}} \cdot \text{m}^{-2} \cdot \text{s}^{-1}$ and $600 \mu\text{mol Photon}_{\text{PAR}} \cdot \text{m}^{-2} \cdot \text{s}^{-1}$).

3.1. One experiment example

First, an example of the experiment is presented to ease the grasp of the concepts at stake. Chlorophyll content (Arbitrary Units) over time

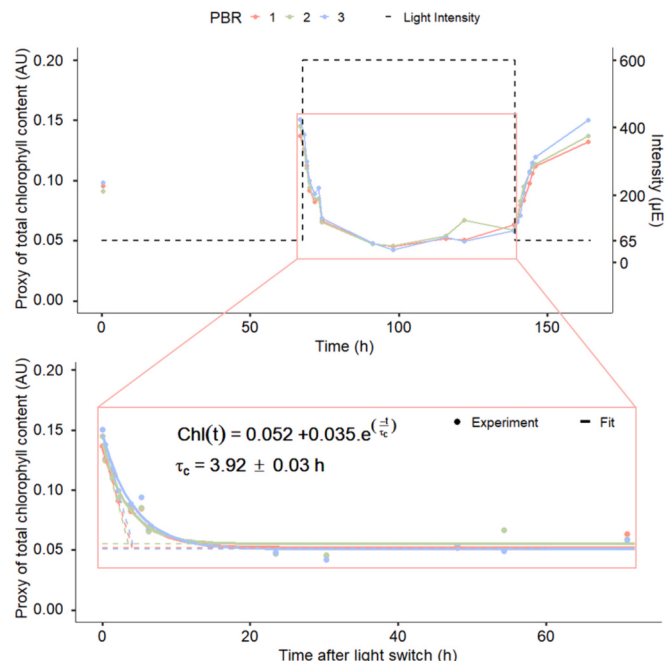
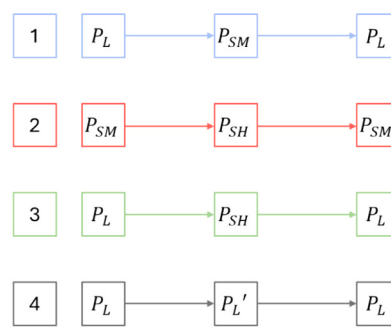


Fig. 4. Upper panel: chlorophyll content over time. Lower panel: focus on the shift from LL to HL and the corresponding fit to an exponential model. The dots represent the experimental values, the lines represent the model. The dashed lines represent the fitted characteristic times τ_c .



for the transitions between $65 \mu\text{mol Photon}_{\text{PAR}} \cdot \text{m}^{-2} \cdot \text{s}^{-1}$ and $600 \mu\text{mol Photon}_{\text{PAR}} \cdot \text{m}^{-2} \cdot \text{s}^{-1}$ is displayed in Fig. 4 (upper panel). This condition corresponds to the most contrasted of all conditions evaluated. The lower panel of Fig. 4 focuses on the transition between *LL* and *HL* and the consequent decrease in chlorophyll content per cell. The fits to the exponential model of Eq. (2) are also represented. The characteristic times of transitions between *LL* and *HL* acclimated states and the acclimated chlorophyll content are underlined respectively by the original tangents and the asymptotes (dashed lines). The first-order model faithfully represents the chlorophyll modulation. No evidence of a lag phase was identified in the chlorophyll modulation after the sudden light change. This example illustrates both the repeatability of the triplicate and the stability of the chlorophyll >24 h after a light shift.

3.2. Acclimated states

Fig. 5 presents the acclimated states of the cultures for the tested intensities in terms of pigment content, carotenoid/chlorophyll ratio, and *PSII* cross-section. The trends of the pigmentary indicators are comparable to literature results [21]. First of all, the chlorophyll content follows the inverse trend of the classical *PI* curve. The three zones P_L , P_{SM} , and P_{SH} were identified. The photolimitation zone is distinctly identifiable given the sharp decrease of chlorophyll content from 0.175 ± 0.007 (arbitrary units) at minimal intensity to 0.094 ± 0.018 at $120 \mu\text{mol Photon}_{\text{PAR}} \cdot \text{m}^{-2} \cdot \text{s}^{-1}$. A more moderate decrease can be observed down to 0.060 ± 0.005 at $300 \mu\text{mol Photon}_{\text{PAR}} \cdot \text{m}^{-2} \cdot \text{s}^{-1}$, which corresponds to the P_{SM} zone. Lastly, the content is statistically unchanged at higher light intensities (corresponding to the P_{SH} zone), averaging 0.062 ± 0.007 between $300 \mu\text{mol Photon}_{\text{PAR}} \cdot \text{m}^{-2} \cdot \text{s}^{-1}$ and $600 \mu\text{mol Photon}_{\text{PAR}} \cdot \text{m}^{-2} \cdot \text{s}^{-1}$.

Total carotenoid content follows the same trend as the chlorophyll content in a lesser proportion, which explains that R_{cc} followed an inverse trend. The delimitation of the light domain in three zones is identifiable but less pronounced. The difficulty of the analysis lies in the

dual role of the carotenoids, some acting as primary harvesting pigments, others being involved in photoprotective mechanisms. The absolute quantity of the first category tends to lower values at *HL*, as it has been shown for lutein in *Scenedesmus obliquus* and *Chlorella vulgaris* [21,46]. On the contrary, carotenoids involved in photoprotective mechanisms (energy dissipation through *NPQ* or *ROS* scavenging) usually accumulate with increasing illumination [26,47]. The trend of total carotenoid content is indicative of the acclimation in terms of light-harvesting capacity, while the trend of R_{cc} highlights the acclimation in terms of photoprotection. The last acclimated state corresponds to the *PSII* cross-section obtained with the fluorometric analysis. The tendency is a downsizing of the cross-section with increasing light intensity, in a considerably less abrupt fashion than for the other indicators. This behavior suggests that the σ -strategy of the algae was activated linearly with the level of light. The overall compatibility of the results in terms of pigments and cross-section with the well-documented acclimated states of green microalgae strengthens the confidence in the validity of the following results.

3.3. Dynamic of acclimation

3.3.1. Pigment modulation

The dynamic of the chlorophyll content modulation in response to the illumination changes was assessed with the exponential model described by Eq. (2). The associated characteristic times τ_c are presented in Fig. 6 (upper panel) as a function of the intensity of acclimation (intensity after the light step). The curve exhibits a pronounced trend of faster transition for higher intensity of acclimation. The data was empirically fitted to a decreasing exponential model, presented as a dashed line. The error and its most likely normal distribution are represented on the lower panel of Fig. 6.

The exponentially decreasing trend is a relevant model for the acclimation times, supported by the statistical analysis of the error. In particular, the error is distributed independently from the category of transition (from *LL* to *HL* or inversely). The decreasing acclimation time

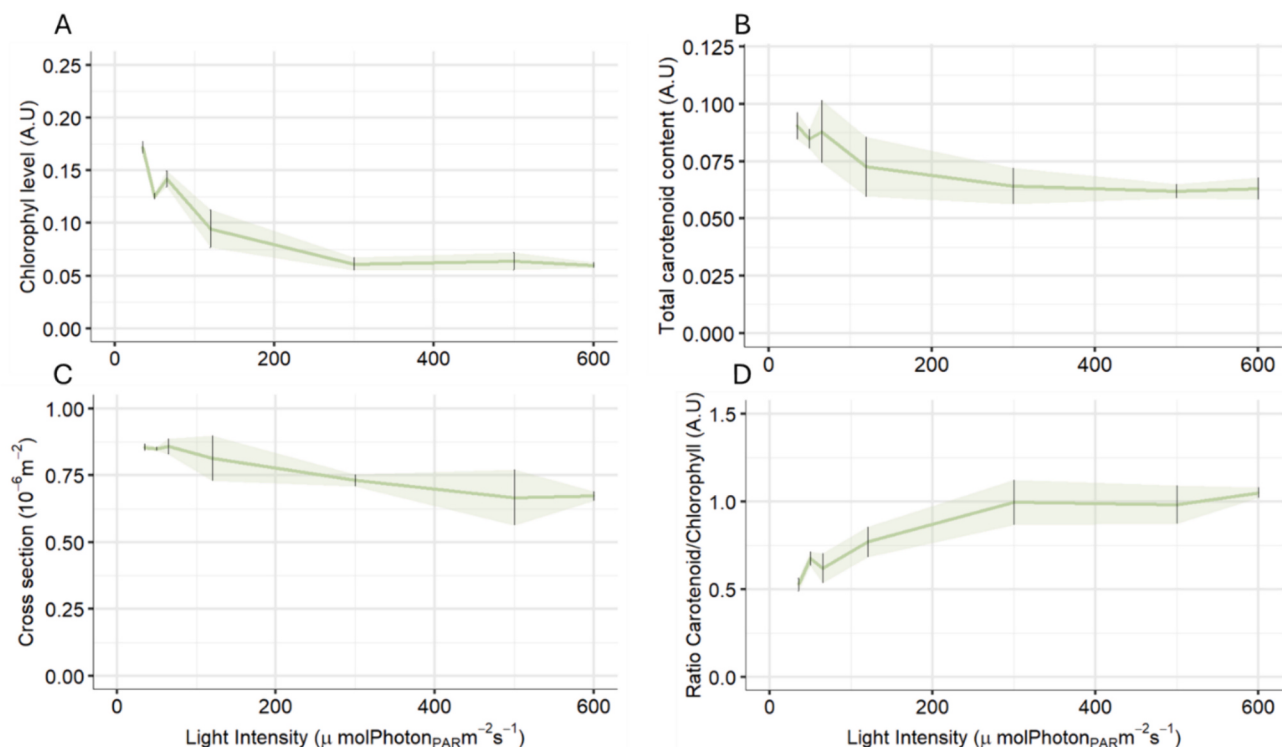


Fig. 5. Biological indicators of algae acclimated to different light intensities. A: Chlorophyll content (Arbitrary Units). B: Carotenoid content (Arbitrary Unit). C: Photosystem II cross-section ($10^{-6} \cdot \text{m}^{-2}$). D: Ratio of carotenoids over chlorophyll content (Arbitrary Units).

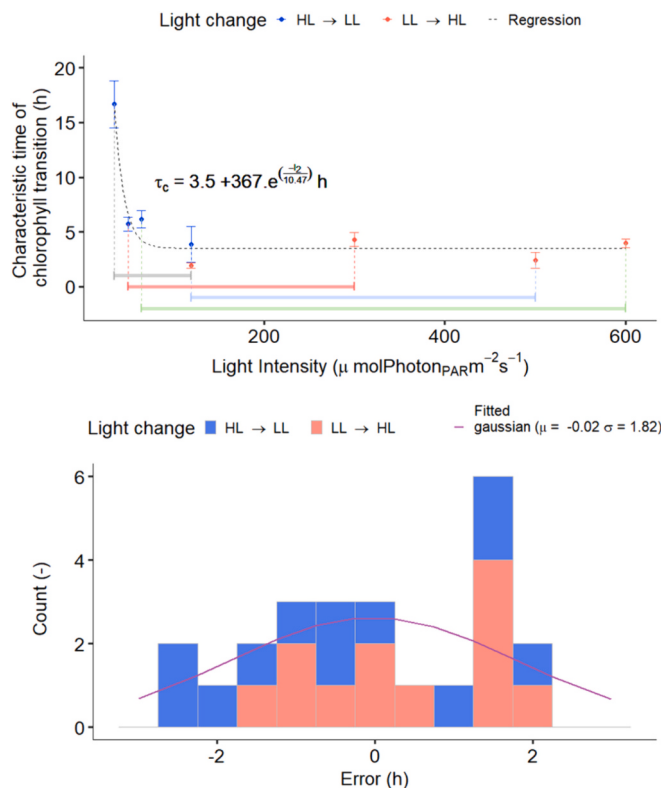


Fig. 6. Upper panel: Characteristic time of chlorophyll content adjustment upon light changes depending on the intensity of acclimation. The equation of the fitted exponential is also presented. Lower panel: Difference between the experimental points and the theoretical exponential calculated on the upper panel. The most likely Gaussian representation of the error is also represented.

with increasing light is also biologically significant, on account of the energetic limitation of photosynthetic microorganisms in low light [48]. In particular, the light-harvesting capacity of the algae is reduced in high light to prevent photodamage to the protein D1 and its repair system [49]. When a transition to low light occurs, the reduced harvesting capacity of *HL*-acclimation combined with a darker environment naturally limits the photon collection. Conversely, when the light is shifted to a higher intensity, the harvesting ability of the *LL*-acclimated algae is magnified, and the photonic collection is eased. This energy is used to diminish the light-harvesting power of the antennae and foster protective mechanisms. This suggests that the starting light intensity (hence the difference between the two levels) affects the acclimation time. The present data suggest that this effect is minor compared to the impact of the light of acclimation, provided that the two light intensities involved are sufficiently different to observe an effective change.

For intensities outside of the photolimitation zone ($I \geq 120 \mu\text{mol Photon}_{\text{PAR}} \cdot \text{m}^{-2} \cdot \text{s}^{-1}$), the characteristic time of acclimation was statistically constant ($\tau_c = 3.55 \pm 1.01 \text{ h}$). In comparison, Shapira et al. found a characteristic time of approximately 6 h after a light shift from $70 \mu\text{mol Photon}_{\text{PAR}} \cdot \text{m}^{-2} \cdot \text{s}^{-1}$ to $700 \mu\text{mol Photon}_{\text{PAR}} \cdot \text{m}^{-2} \cdot \text{s}^{-1}$ for *Chlamydomonas reinhardtii* [32]. These results constitute an indication of an energetic limitation in the acclimation of green microalgae and provide consistent values of acclimation time for intensities of the photo-saturation zone.

One should note that the empirical model of the decreasing exponential does not extend to extreme intensities for which other phenomena come into play (principally photodamage and repair mechanisms in exceedingly high light (above at least $800 \mu\text{mol Photon}_{\text{PAR}} \cdot \text{m}^{-2} \cdot \text{s}^{-1}$ for *Chlorella vulgaris* [21]) and respiration in extremely low light (below $10 \mu\text{mol Photon}_{\text{PAR}} \cdot \text{m}^{-2} \cdot \text{s}^{-1}$ for *Chlorella vulgaris* [50]).

3.3.2. Photosynthetic apparatus

The photoacclimation mechanisms of the microalgae encompass more than the sole modification of the light-harvesting ability, which can itself be achieved through different mechanisms. Fluorescence measurements provided more in-depth insights into the acclimation processes pertaining to the photosynthetic apparatus. Fig. 7 and Fig. 8 present the different fluorometric indicators for four shifts. The first rows represent the quantum efficiencies T_0/ABS , TR_0/ABS , and ET_0/TR_0 . The middle rows represent the phenomenological ratios ABS/CS_0 , TR_0/CS_0 , ET_0/CS_0 , and RC/CS_0 , the last ones represent the cross-section σ_{PSII} .

For the first condition (transitions between 35 and $120 \mu\text{mol Photon}_{\text{PAR}} \cdot \text{m}^{-2} \cdot \text{s}^{-1}$), most indicators remained constant. In the transition from *LL* to *HL*, the absorption per excited cross-section and trapping per excited cross-section slightly decreased, parallelly to the chlorophyll content. This suggests that the acclimation essentially concerns the antennae's ability to collect and transfer light to the special pair, either by modulating the antenna size (quantity of pigment bound to the light-harvesting complexes [51]) or the geometrical arrangement of the pigments that constitute it [52]. The opposite transition (*HL* to *LL*) did not exhibit a sensible difference in most indicators for the first 8 hours, except the *PSII* cross-section that decreased from $(0.860 \pm 0.010) \times 10^{-6} \text{ m}^{-2}$ to $(0.825 \pm 0.002) \times 10^{-6} \text{ m}^{-2}$ before returning to the initial value $(0.876 \pm 0.027) \times 10^{-6} \text{ m}^{-2}$ after 24 h. Overall, most indicators remained statistically constant throughout the two successive light changes, which reflects the similarity of the photosynthetic apparatus of the microalgae acclimated to these two intensities of the photolimitation zone.

The second condition showed a different and contrasted behavior. For the transition from $65 \mu\text{mol Photon}_{\text{PAR}} \cdot \text{m}^{-2} \cdot \text{s}^{-1}$ to $600 \mu\text{mol Photon}_{\text{PAR}} \cdot \text{m}^{-2} \cdot \text{s}^{-1}$, the value of TR_0/ABS (commonly presented in the literature as $\frac{F_u}{F_m}$) followed a noticeable decrease from 0.736 ± 0.012 to 0.626 ± 0.019 in three hours, before starting to recover after approximatively 6 h and finally reach back its initial value $< 24 \text{ h}$ after the light shift. This is, along with the steep decrease of the three phenomenological fluxes (second row), an indication of the effect of this intense light increase. ET_0/CS_0 stayed constant, showing that the photoprotective mechanisms allowed the algae to cope and the photosynthetic apparatus to function at the maximum of its possibility throughout the experiment. In the meantime, the number of reaction centers per excited cross-section slightly increased from 0.095 ± 0.009 to 0.133 ± 0.057 within the first eight hours, before reducing to 0.040 ± 0.008 (final value after 72 h) hinting towards an acclimation in two steps. The first step most likely corresponded to a σ -strategy, where the cross-section decreased with a constant (or more slowly evolving) number of reaction centers. The second step resembled an N -strategy, with a decrease in the number of reaction centers per excited cross-section.

On the inverse transition (from $600 \mu\text{mol Photon}_{\text{PAR}} \cdot \text{m}^{-2} \cdot \text{s}^{-1}$ to $65 \mu\text{mol Photon}_{\text{PAR}} \cdot \text{m}^{-2} \cdot \text{s}^{-1}$), all phenomenological fluxes increased more or less pronouncedly, along with the *PSII* cross-section. The quantum efficiencies were very stable, which translates the fact that the whole apparatus was evolving concomitantly. The dynamic of the phenomenological fluxes was slightly more complex, and three phases could be identified regarding their evolution. First, all indicators (ABS/CS_0 , TR_0/CS_0 , ET_0/CS_0 , and RC/CS_0) increased and reached a maximum after approximately 6 h. Secondly, they experienced a sharp decrease during the three following hours (8 h after the light shift). Lastly, the indicators were statistically constant for the 16 following hours (24 h after the light shift). The two first phases reflect a two-step strategy of acclimation of the algae to increase its light-harvesting ability. The initial phase most likely corresponds to a predominance of an N -strategy regarding the marked increase of RC/CS_0 . This increase corresponds either to an increase in the absolute number of reaction centers, a decrease in the excited cross-section, or both. In the second

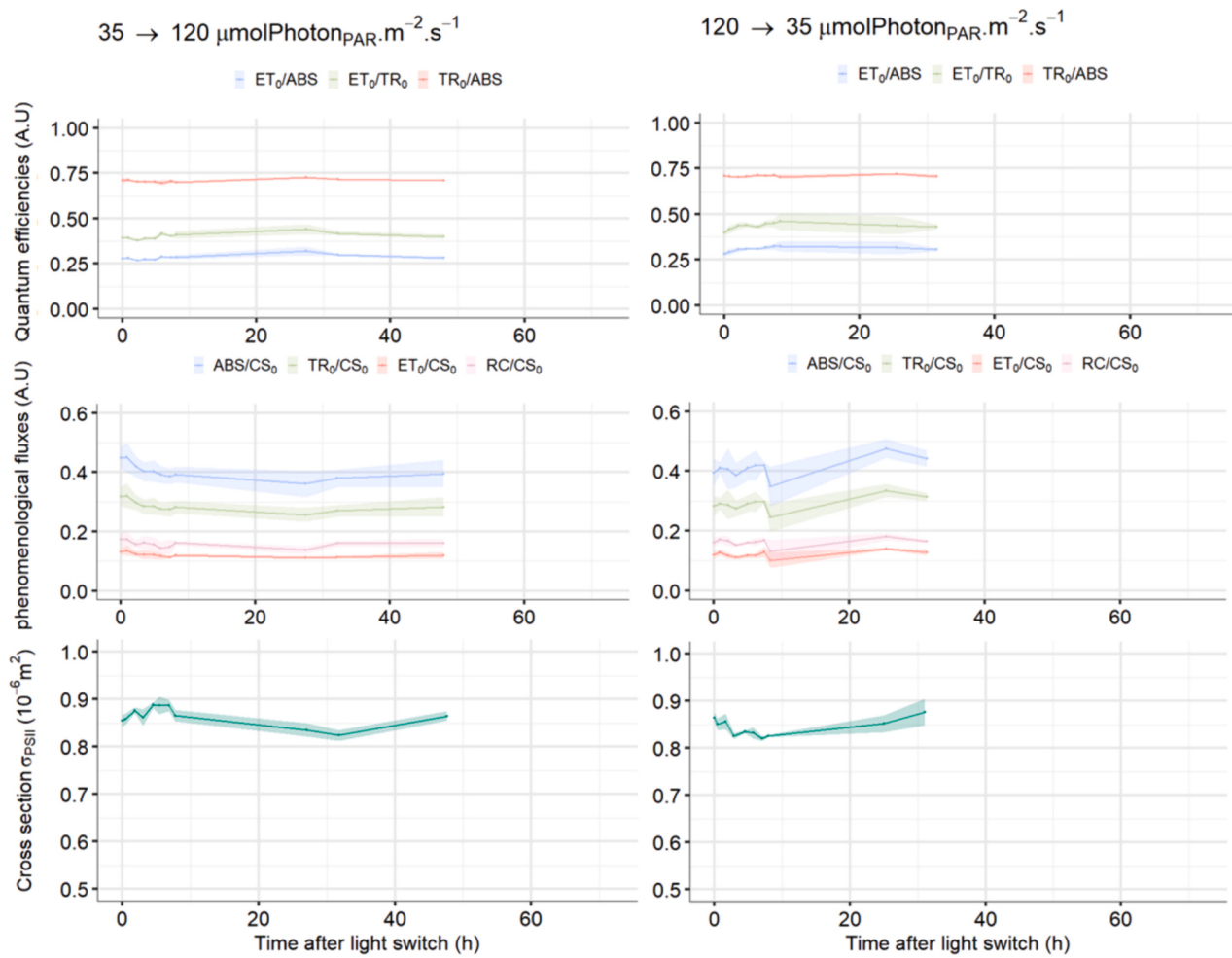


Fig. 7. Fluorometric indicators (first part). First row: Phenomenological fluxes in arbitrary units. Middle row: Quantum efficiencies in arbitrary units. Last row: Cross-section of Photosystem II ($10^{-6} \cdot m^2$).

phase, the number of reaction centers per excited cross-section decreased, indicative of the σ -strategy adopted by the algae. The behavior of the parameters during this second phase suggests that both the number of active reaction centers and the cross-section were increasing during the 8 h with different proportions and dynamics.

The evolution of σ_{PSII} for the other conditions (not presented) was for the most part similar to what is observable for the transitions between $65 \mu\text{mol Photon}_{\text{PAR}} \cdot \text{m}^{-2} \cdot \text{s}^{-1}$ and $600 \mu\text{mol Photon}_{\text{PAR}} \cdot \text{m}^{-2} \cdot \text{s}^{-1}$. The $PSII$ cross-section evolved linearly (and inversely to the light shift) during 24 to 48 h and remained constant afterward. This modulation dynamic was overall slower than the one of chlorophyll content exhibited by the algae.

3.4. Hysteresis effect

In addition to the acclimation mechanisms, the data allowed the absence of any hysteresis effect to be highlighted. Fig. 9 presents the acclimated values of the three main indicators (chl , R_{cc} , and σ_{PSII}) before and after two successive shifts. One of the pairs did not qualify for the analysis (Bartlett test $p > 0.05$). On the 8 remaining pairs, only σ_{PSII} at $65 \mu\text{mol Photon}_{\text{PAR}} \cdot \text{m}^{-2} \cdot \text{s}^{-1}$ was statistically different between the beginning and the end of the experiment. Regarding the trend of the corresponding curve presented in Fig. 8, this difference may stem from an unfinished transition rather than a difference in acclimated cross-section. Otherwise, the difference in cross-sections could be explained by the two-phase acclimation (N and σ strategies) revealed by the OJIP

assays. The remaining comparisons corroborate the fact that microalgae adjust their photosynthetic machinery to illumination without a memory of the previously experienced light. In particular, the dynamic of acclimation depends on the available light at the moment. For transitions between two illuminations not burdened by energetic limitations, the chlorophyll content transits between two fixed values with a comparable dynamic. One should note that these results do not suffice to conclude about the absence of a hysteresis effect in the case of extremely high light intensities that can induce photo-damage.

4. Discussion

The dynamic of acclimation of *Chlorella vulgaris* was highlighted by the evolution of the chlorophyll content over time and comforted by the consistency of the fluorometric measurements. However, some limitations of the study must be addressed.

First of all, the results in acclimated states were closer to the literature for *LL* than for *HL* conditions. A difference of 66 % between $35 \mu\text{mol Photon}_{\text{PAR}} \cdot \text{m}^{-2} \cdot \text{s}^{-1}$ and $300 \mu\text{mol Photon}_{\text{PAR}} \cdot \text{m}^{-2} \cdot \text{s}^{-1}$ was measured, very close to the decrease of 68 % obtained with a similar strain and *PBR* between these same intensities [21]. However, while the decline continued in the literature (82% decrease between $35 \mu\text{mol Photon}_{\text{PAR}} \cdot \text{m}^{-2} \cdot \text{s}^{-1}$ and $600 \mu\text{mol Photon}_{\text{PAR}} \cdot \text{m}^{-2} \cdot \text{s}^{-1}$), it stayed constant in the present study (Fig. 5). One should note that it is virtually impossible to compare the characteristic time of antenna modulation with the literature, due to both the scarcity of available data and the

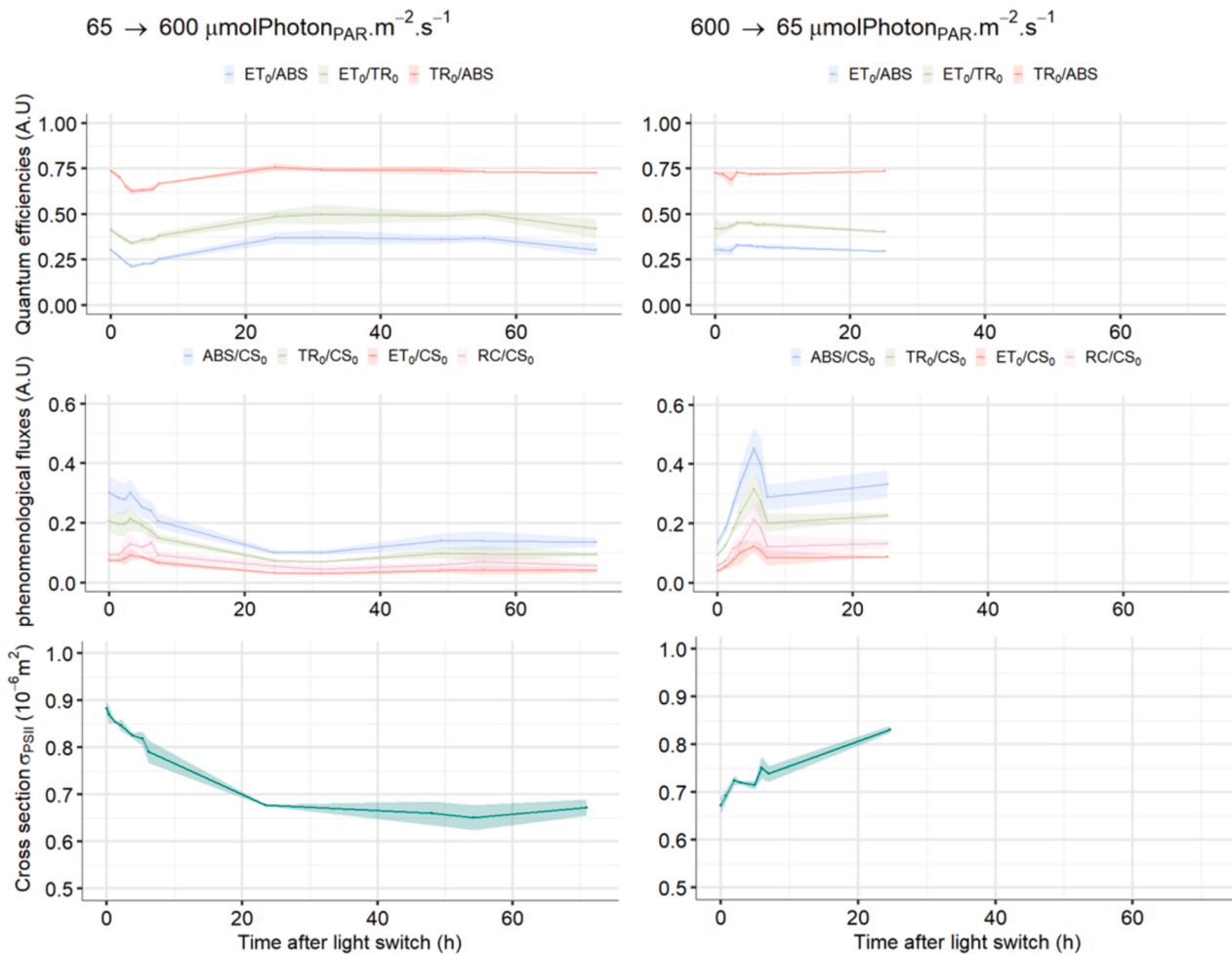


Fig. 8. Fluorometric indicators (second part). First row: Phenomenological fluxes in arbitrary units. Middle row: Quantum efficiencies in arbitrary units. Last row: Cross-section of Photosystem II ($10^{-6} \cdot m^{-2}$).

difference in the experimental protocols (strain, light intensities, nature of the indicators).

Secondly, the fluorometric measurements helped validate the preceding conclusions but did not exhibit a consistent behavior among all transitions. The data highlighted a σ -acclimation strategy for all light intensities, linearly scaled with the intensity. N -strategies of acclimation were only observable for transitions involving intensities significantly higher than I_L . In this case, the results highlighted a symmetrical two-step strategy. When changing the light from LL to HL , the σ -strategy was favored in the first phase and the N -strategy in the second. The inverse occurrence was observed for the transition from HL to LL (N -strategy followed by a σ -strategy). These results represent a potential indication of a prioritization system between one or the other strategy based on the illumination and acclimated states. However, more data would be necessary to untangle with precision the acclimation strategies and identify conditions that foster one over the other. Lastly, the modulation in σ_{PSII} did not systematically follow an exponential behavior but was consistently slower than the pigment modulation. One possible hypothesis relies on the evolution of the $PSII - PSI$ stoichiometry which takes place over a longer time scale than antenna size modulation [53]. As the number of $PSII$ increases with the acclimation to high light and the harvesting ability lowers, σ_{PSII} decreases (lower photosystem closing rate). A qualification of the PSI cross-section would be necessary to assess the validity of this theory.

A last point should be underlined, concerning the carotenoid data. The subtraction method proposed here did not allow to differentiate between carotenoids, which rendered the analysis of photoprotective

mechanisms complex, if not impossible. Carotenoids have a dual role in light harvesting and photoprotection in green microalgae, and their dynamic of acclimation varies greatly depending on their role in the photosynthetic apparatus. The proxy of carotenoid content and the ratio of carotenoid relative to chlorophyll gave an insight into the acclimated states of the algae (Fig. 5). However, analyzing their dynamic would require further information on the carotenoid profiles to untangle the concurrent mechanisms. Accessing the carotenoid profile with a similar acquisition frequency would pose many challenges, mostly related to the difficulty of increasing the volume of culture while keeping a short light path and low optical density, both required to ensure a quasi-uniform light intensity.

The results of this study confirm that green microalgae can adjust their antenna size in a few hours, provided sufficient energy is available. This has direct consequences on scale-up or fed-batch culture management. In the former, the process implies at one point inoculating small quantities of microalgae in *PBRs*, resulting in a low concentrated culture, with low optical density and high light availability for the few cells remaining. In the latter, part of the culture is removed and replaced by a fresh medium, resulting in identical consequences. The acclimation dynamic in both cases is dictated by the light availability in the diluted culture. Hence, the algae quantity to respectively inoculate and sample can be fine-tuned to optimize transitions. Similarly, the difference in acclimation dynamics exhibited by this study can be useful in addressing the acclimated states of microalgae in dense culture, especially considering the uneven dimensions of photic and aphotic zones within a *PBR* and the difference in acclimation dynamics related to the illumination.

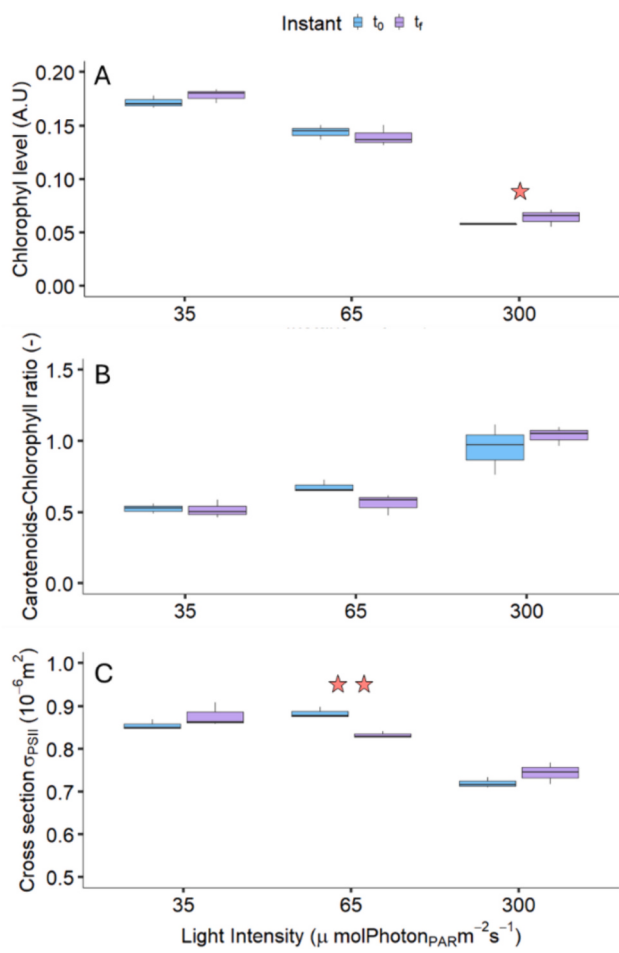


Fig. 9. Comparison of Chlorophyll content (A), Carotenoid/chlorophyll ratio (B), and cross-section (C) at the beginning and the end of experiments involving two successive shifts. One star indicates a difference in the variance (Bartlett test $p > 0.05$), and two stars indicate a difference in the means (ANOVA test $p > 0.05$).

In particular, the energetic limitation in low light must be addressed when estimating acclimation to intermittent light conditions generated by mixing in dense cultures.

5. Conclusion

Photo-acclimation of the green algae *Chlorella vulgaris* was monitored for eight different light transitions, up and down, between intensities ranging from $35 \mu\text{mol Photon}_{\text{PAR}}\text{m}^{-2}\text{s}^{-1}$ to $600 \mu\text{mol Photon}_{\text{PAR}}\text{m}^{-2}\text{s}^{-1}$. The acclimated values of pigment content were consistent with the literature. A pronounced difference in characteristic time of chlorophyll modulation at the lowest intensity compared to higher illuminations indicated an energetic limitation in the photoacclimation process. The dynamic of acclimation of *Chlorella vulgaris* is primarily dictated by the intensity to which the algae acclimates while the previous light intensity is of secondary importance. The exponentially decreasing trend of the characteristic transition time of chlorophyll content between 35 and $120 \mu\text{mol Photon}_{\text{PAR}}\text{m}^{-2}\text{s}^{-1}$ to a constant level was consistent with the delimitation of the light intensities into photolimitation and photo-saturation zones. These conclusions were corroborated by fluorometric measurements consistent with the knowledge about photoprotective mechanisms. In addition, these fluorometric assays indicated a linear relation between σ -strategy and illumination level and highlighted an additional N -strategy for transitions between photolimitation and high-light photo-saturation

zone. Lastly, no hysteresis effect was observable for the pigment and fluorometric indicators considering cycles of two successive light shifts. Altogether, this study provides consistent information on the dynamic of photoacclimation from a biotechnological standpoint and could help design acclimation models, as well as strategies for cultures and scale-up.

CRediT authorship contribution statement

Arthur Oliver: Writing – original draft, Methodology, Investigation, Formal analysis, Conceptualization. **Patrick Perré:** Writing – review & editing, Validation, Funding acquisition, Formal analysis, Conceptualization. **Victor Pozzobon:** Writing – review & editing, Validation, Supervision, Formal analysis, Conceptualization.

Declaration of competing interest

The authors declare that they have no known competing financial interests or personal relationships that could have appeared to influence the work reported in this paper.

Data availability

Data will be made available on request.

Acknowledgment

Communauté urbaine du Grand Reims, Département de la Marne, Région Grand Est and European Union (FEDER Grand Est 2021-2027) are acknowledged for their financial support to the Chair of Biotechnology of CentraleSupélec and the Centre Européen de Biotechnologie et de Bioéconomie (CEBB).

Appendix A. Supplementary data

Supplementary data to this article can be found online at <https://doi.org/10.1016/j.algal.2024.103661>.

References

- [1] W. Levasseur, P. Perré, V. Pozzobon, A review of high value-added molecules production by microalgae in light of the classification, *Biotechnol. Adv.* 41 (2020) 107545, <https://doi.org/10.1016/j.biotechadv.2020.107545>.
- [2] Y. Maltsev, K. Maltseva, Fatty acids of microalgae: diversity and applications, *Rev. Environ. Sci. Biotechnol.* 20 (2021) 515–547, <https://doi.org/10.1007/s11157-021-09571-3>.
- [3] M. Plöhn, O. Spain, S. Sirin, M. Silva, C. Escudero-Oñate, L. Ferrando-Climent, Y. Allahverdiyeva, C. Funk, Wastewater treatment by microalgae, *Physiol. Plant.* 173 (2021) 568–578, <https://doi.org/10.1111/ppl.13427>.
- [4] M.T. Ahmad, M. Shariff, F.Md. Yusoff, Y.M. Goh, S. Banerjee, Applications of microalgae *Chlorella vulgaris* in aquaculture, *Rev. Aquac.* 12 (2020) 328–346, <https://doi.org/10.1111/raq.12320>.
- [5] L. Gouveia, A.P. Batista, I. Sousa, A. Raymundo, N.M. Bandarra, Microalgae in novel food products. In Papadopoulos, K. - Food Chemistry Research Developments. Nova Science Publishers (2008) 75–112.
- [6] J.C. Ogbonna, H. Masui, H. Tanaka, Sequential heterotrophic/autotrophic cultivation – an efficient method of producing *Chlorella* biomass for health food and animal feed, *J. Appl. Phycol.* 9 (1997) 359–366, <https://doi.org/10.1023/A:1007981930676>.
- [7] J. Ruiz, R.H. Wijffels, M. Dominguez, M.J. Barbosa, Heterotrophic vs autotrophic production of microalgae: bringing some light into the everlasting cost controversy, *Algal Res.* 64 (2022) 102698, <https://doi.org/10.1016/j.algal.2022.102698>.
- [8] S.N. Chanquia, G. Vernet, S. Kara, Photobioreactors for cultivation and synthesis: specifications, challenges, and perspectives, *Eng. Life Sci.* 22 (2022) 712–724, <https://doi.org/10.1002/elsc.202100070>.
- [9] S.K. Ratha, R. Prasanna, Bioprospecting microalgae as potential sources of “green energy”—challenges and perspectives (review), *Appl. Biochem. Microbiol.* 48 (2012) 109–125, <https://doi.org/10.1134/S000368381202010X>.
- [10] M.R. Tredici, G.C. Zittelli, Efficiency of sunlight utilization: tubular versus flat photobioreactors, *Biotechnol. Bioeng.* 57 (1998) 187–197, [https://doi.org/10.1002/\(SICI\)1097-0290\(19980120\)57:2<187::AID-BIT7>3.0.CO;2-J](https://doi.org/10.1002/(SICI)1097-0290(19980120)57:2<187::AID-BIT7>3.0.CO;2-J).
- [11] A.P. Carvalho, S.O. Silva, J.M. Baptista, F.X. Malcata, Light requirements in microalgal photobioreactors: an overview of biophotonic aspects, *Appl. Microbiol. Biotechnol.* 89 (2011) 1275–1288, <https://doi.org/10.1007/s00253-010-3047-8>.

- [12] C. Martínez, F. Mairet, O. Bernard, Theory of turbid microalgae cultures, *J. Theor. Biol.* 456 (2018) 190–200, <https://doi.org/10.1016/j.jtbi.2018.07.016>.
- [13] V. Pozzobon, *Chlorella vulgaris* cultivation under super high light intensity: an application of the flashing light effect, *Algal Res.* 68 (2022) 102874, <https://doi.org/10.1016/j.algal.2022.102874>.
- [14] Z. Khoobkar, F.P. Shariati, A.A. Safekordi, H.D. Amrei, Performance assessment of a novel pyramid Photobioreactor for cultivation of microalgae using external and internal light sources, *Food Technol. Biotechnol.* 57 (2019) 68–76, <https://doi.org/10.17113/fbt.57.01.19.5702>.
- [15] I.S. Suh, S.B. Lee, A light distribution model for an internally radiating photobioreactor, *Biotechnol. Bioeng.* 82 (2003) 180–189, <https://doi.org/10.1002/bit.10558>.
- [16] M. Heining, A. Sutor, S.C. Stute, C.P. Lindenberger, R. Buchholz, Internal illumination of photobioreactors via wireless light emitters: a proof of concept, *J. Appl. Phycol.* 27 (2015) 59–66, <https://doi.org/10.1007/s10811-014-0290-x>.
- [17] R. Laifa, J. Morchain, L. Barna, P. Guiraud, A numerical framework to predict the performances of a tubular photobioreactor from operating and sunlight conditions, *Algal Res.* 60 (2021) 102550, <https://doi.org/10.1016/j.algal.2021.102550>.
- [18] W. Levasseur, V. Pozzobon, P. Perré, Green microalgae in intermittent light: a meta-analysis assisted by machine learning, *J. Appl. Phycol.* 34 (2022) 135–158, <https://doi.org/10.1007/s10811-021-02603-z>.
- [19] C. Vejrazka, M. Janssen, M. Streefland, R.H. Wijffels, Photosynthetic efficiency of *Chlamydomonas reinhardtii* in attenuated, flashing light, *Biotechnol. Bioeng.* 109 (2012) 2567–2574, <https://doi.org/10.1002/bit.24525>.
- [20] S. Lima, P.S.C. Schulze, I.M. Schüller, R. Rautenberger, D. Morales-Sánchez, T. F. Santos, H. Pereira, J.C.S. Varela, F. Scargiali, R.H. Wijffels, V. Kiron, Flashing light emitting diodes (LEDs) induce proteins, polyunsaturated fatty acids and pigments in three microalgae, *J. Biotechnol.* 325 (2021) 15–24, <https://doi.org/10.1016/j.jbiotec.2020.11.019>.
- [21] W. Levasseur, P. Perré, V. Pozzobon, *Chlorella vulgaris* acclimated cultivation under flashing light: an in-depth investigation under iso-actinic conditions, *Algal Res.* 70 (2023) 102976, <https://doi.org/10.1016/j.algal.2023.102976>.
- [22] R.J. Geider, H.L. MacIntyre, T.M. Kana, A dynamic regulatory model of phytoplanktonic acclimation to light, nutrients, and temperature, *Limnol. Oceanogr.* 43 (1998) 679–694, <https://doi.org/10.4319/lo.1998.43.4.0679>.
- [23] Z.U. Rehman, A.K. Anal, Enhanced lipid and starch productivity of microalga (<i>Chlorococcum</i> sp. <i>TISTR 8583</i>) with nitrogen limitation following effective pretreatments for biofuel production, *Biotechnol. Rep. (Amst.)* 21 (2018) e00298. doi:<https://doi.org/10.1016/j.btre.2018.e00298>.
- [24] B. Xu, P. Cheng, C. Yan, H. Pei, W. Hu, The effect of varying LED light sources and influent carbon/nitrogen ratios on treatment of synthetic sanitary sewage using *Chlorella vulgaris*, *World J. Microbiol. Biotechnol.* 12 (2013).
- [25] T. Fisher, J. Minnaard, Z. Dubinsky, Photoacclimation in the marine alga *Nannochloropsis* sp. (eustigmatophyte): a kinetic study, *J. Plankton Res.* (1996) 1797–1818.
- [26] P. Müller, X.-P. Li, K.K. Niyogi, Non-photochemical quenching, A Response to Excess Light Energy, *Plant Physiology* 125 (2001) 1558–1566, <https://doi.org/10.1104/pp.125.4.1558>.
- [27] N.I. Krinsky, in: T.W. Goodwin (Ed.), CAROTENOID PROTECTION AGAINST OXIDATION, Carotenoids C5, Pergamon, 1979, pp. 649–660, <https://doi.org/10.1016/B978-0-08-022359-9.50018-7>.
- [28] A. Telfer, What is β-carotene doing in the photosystem II reaction Centre? *Philos. Trans. R. Soc. Lond. B* 357 (2002) 1431–1440, <https://doi.org/10.1098/rstb.2002.1139>.
- [29] Z. Amini Khoeyi, J. Seyfabadi, Z. Ramezanpour, Effect of light intensity and photoperiod on biomass and fatty acid composition of the microalgae, *Chlorella vulgaris*, *Aquac. Int.* 20 (2012) 41–49, <https://doi.org/10.1007/s10499-011-9440-1>.
- [30] S.L. Meseck, J.H. Alix, G.H. Wikfors, Photoperiod and light intensity effects on growth and utilization of nutrients by the aquaculture feed microalga, *Tetraselmis chui* (PLY429), *Aquaculture* 246 (2005) 393–404, <https://doi.org/10.1016/j.aquaculture.2005.02.034>.
- [31] T. Fisher, T. Berner, D. Iluz, Z. Dubinsky, The kinetics of the Photoacclimation response of *Nannochloropsis* sp. (eustigmatophyceae): a study of changes in ultrastructure and P_{st} density, *J. Phycol.* 34 (1998) 818–824, <https://doi.org/10.1046/j.1529-8817.1998.340818.x>.
- [32] M. Shapira, A. Lers, P.B. Heifetz, V. Irihimovitz, C. Barry Osmond, N.W. Gillham, J. E. Boynton, Differential regulation of chloroplast gene expression in *Chlamydomonas reinhardtii* during photoacclimation: light stress transiently suppresses synthesis of the rubisco LSU protein while enhancing synthesis of the PS II D1 protein, *Plant Mol. Biol.* 33 (1997) 1001–1010, <https://doi.org/10.1023/A:1005814800641>.
- [33] L. Straka, B.E. Rittmann, Dynamic response of *Synechocystis* sp. PCC 6803 to changes in light intensity, *Algal Res.* 32 (2018) 210–220, <https://doi.org/10.1016/j.algal.2018.04.004>.
- [34] T. de Mooij, Z.R. Nejad, L. van Buren, R.H. Wijffels, M. Janssen, Effect of photoacclimation on microalgae mass culture productivity, *Algal Res.* 22 (2017) 56–67, <https://doi.org/10.1016/j.algal.2016.12.007>.
- [35] A. Nikolaou, P. Hartmann, A. Sciandra, B. Chachuat, O. Bernard, Dynamic coupling of photoacclimation and photoinhibition in a model of microalgae growth, *J. Theor. Biol.* 390 (2016) 61–72, <https://doi.org/10.1016/j.jtbi.2015.11.004>.
- [36] F. García-Camacho, A. Sánchez-Mirón, E. Molina-Grima, F. Camacho-Rubio, J. C. Merchuk, A mechanistic model of photosynthesis in microalgae including photoacclimation dynamics, *J. Theor. Biol.* 304 (2012) 1–15, <https://doi.org/10.1016/j.jtbi.2012.03.021>.
- [37] L. Straka, B.E. Rittmann, Light attenuation changes with photo-acclimation in a culture of *Synechocystis* sp. PCC 6803, *Algal Res.* 21 (2017) 223–226, <https://doi.org/10.1016/j.algal.2016.11.024>.
- [38] R.A. Andersen, *Algal Culturing Techniques*, Academic Press, 2005.
- [39] R.J. Porra, A simple method for extracting chlorophylls from the recalcitrant alga, *Nannochloris atomus*, without formation of spectroscopically-different magnesium-rhodochlorin derivatives, *Biochimica et Biophysica Acta (BBA), Bioenergetics* 1019 (1990) 137–141, [https://doi.org/10.1016/0005-2728\(90\)90135-Q](https://doi.org/10.1016/0005-2728(90)90135-Q).
- [40] M. Taniguchi, J.S. Lindsey, Absorption and fluorescence spectral database of chlorophylls and analogues, *Photochem. Photobiol.* 97 (2021) 136–165, <https://doi.org/10.1111/php.13319>.
- [41] J. Lavergne, E. Leci, Properties of inactive photosystem II centers, *Photosynth. Res.* 35 (1993) 323–343, <https://doi.org/10.1007/BF00016563>.
- [42] A. Melis, J.M. Anderson, Structural and functional organization of the photosystems in spinach chloroplasts. Antenna size, relative electron-transport capacity, and chlorophyll composition, *Biochimica et Biophysica Acta (BBA), Bioenergetics* 724 (1983) 473–484, [https://doi.org/10.1016/0005-2728\(83\)90108-1](https://doi.org/10.1016/0005-2728(83)90108-1).
- [43] A. Melis, P.H. Homann, Heterogeneity of the photochemical centers in system ii of chloroplasts*, *Photochem. Photobiol.* 23 (1976) 343–350, <https://doi.org/10.1111/j.1751-1097.1976.tb07259.x>.
- [44] R. Strasser, A. Srivastava, M. Tsimilli-Michael, *The Fluorescence Transient as a Tool to Characterize and Screen Photosynthetic Samples, Mechanism, Regulation and Adaptation, Probing Photosynthesis*, 2000.
- [45] W. Levasseur, Biotechnological Performances of Acclimated Green Microalgae Cultures: Effect of Light and its Modulations, n.d.
- [46] S.-H. Ho, M.-C. Chan, C.-C. Liu, C.-Y. Chen, W.-L. Lee, D.-J. Lee, J.-S. Chang, Enhancing lutein productivity of an indigenous microalga *Scenedesmus obliquus* FSP-3 using light-related strategies, *Bioresour. Technol.* 152 (2014) 275–282, <https://doi.org/10.1016/j.biortech.2013.11.031>.
- [47] V. Henríquez, C. Escobar, J. Galarraga, J. Gimel, Carotenoids in Microalgae, Sub-Cellular Biochemistry, in: 2016, pp. 219–237, https://doi.org/10.1007/978-3-319-39126-7_8.
- [48] D.A. Walker, Biofuels, facts, fantasy, and feasibility, *J. Appl. Phycol.* 21 (2009) 509–517, <https://doi.org/10.1007/s10811-009-9446-5>.
- [49] K. Das, A. Roychoudhury, Reactive oxygen species (ROS) and response of antioxidants as ROS-scavengers during environmental stress in plants, *Front. Environ. Sci.* 2 (2014). <https://doi.org/10.3389/fenvs.2014.00053> (accessed December 19, 2022).
- [50] J. Degen, A. Uebel, A. Retze, U. Schmid-Staiger, W. Trösch, A novel airlift photobioreactor with baffles for improved light utilization through the flashing light effect, *J. Biotechnol.* 92 (2001) 89–94, [https://doi.org/10.1016/S0168-1656\(01\)00350-9](https://doi.org/10.1016/S0168-1656(01)00350-9).
- [51] L. Guidi, M. Tattini, M. Landi, How does chloroplast protect chlorophyll against excessive light? *Chlorophyll* (2017) <https://doi.org/10.5772/67887>.
- [52] M. Sener, J. Strümpter, J. Hsin, D. Chandler, S. Scheuring, C.N. Hunter, K. Schulten, Förster energy transfer theory as reflected in the structures of photosynthetic light-harvesting systems, *ChemPhysChem* 12 (2011) 518–531, <https://doi.org/10.1002/cphc.201000944>.
- [53] E. Erickson, S. Wakao, K.K. Niyogi, Light stress and photoprotection in *Chlamydomonas reinhardtii*, *Plant J.* 82 (2015) 449–465, <https://doi.org/10.1111/tpj.12825>.